RESEARCH ARTICLE

Efficacy and Safety of Abemaciclib, an Inhibitor of CDK4 and CDK6, for Patients with Breast Cancer, Non–Small Cell Lung Cancer, and Other Solid Tumors

Amita Patnaik[1], Lee S. Rosen[2], Sara M. Tolaney[3], Anthony W. Tolcher[1], Jonathan W. Goldman[2], Leena Gandhi[3], Kyriakos P. Papadopoulos[1], Muralidhar Beeram[1], Drew W. Rasco[1], John F. Hilton[3], Aejaz Nasir[4], Richard P. Beckmann[4], Andrew E. Schade[4], Angie D. Fulford[4], Tuan S. Nguyen[4], Ricardo Martinez[4], Palaniappan Kulanthaivel[4], Lily Q. Li[4], Martin Frenzel[4], Damien M. Cronier[4], Edward M. Chan[4], Keith T. Flaherty[5], Patrick Y. Wen[3], and Geoffrey I. Shapiro[3]

ABSTRACT We evaluated the safety, pharmacokinetic profile, pharmacodynamic effects, and antitumor activity of abemaciclib, an orally bioavailable inhibitor of cyclin-dependent kinases (CDK) 4 and 6, in a multicenter study including phase I dose escalation followed by tumor-specific cohorts for breast cancer, non–small cell lung cancer (NSCLC), glioblastoma, melanoma, and colorectal cancer. A total of 225 patients were enrolled: 33 in dose escalation and 192 in tumor-specific cohorts. Dose-limiting toxicity was grade 3 fatigue. The maximum tolerated dose was 200 mg every 12 hours. The most common possibly related treatment-emergent adverse events involved fatigue and the gastrointestinal, renal, or hematopoietic systems. Plasma concentrations increased with dose, and pharmacodynamic effects were observed in proliferating keratinocytes and tumors. Radiographic responses were achieved in previously treated patients with breast cancer, NSCLC, and melanoma. For hormone receptor–positive breast cancer, the overall response rate was 31%; moreover, 61% of patients achieved either response or stable disease lasting ≥6 months.

SIGNIFICANCE: Abemaciclib represents the first selective inhibitor of CDK4 and CDK6 with a safety profile allowing continuous dosing to achieve sustained target inhibition. This first-in-human experience demonstrates single-agent activity for patients with advanced breast cancer, NSCLC, and other solid tumors. *Cancer Discov; 6(7); 740–53. ©2016 AACR.*

See related commentary by Lim et al., p. 697.

[1]South Texas Accelerated Research Therapeutics, San Antonio, Texas. [2]University of California, Los Angeles, California. [3]Dana-Farber Cancer Institute, Boston, Massachusetts. [4]Eli Lilly and Company, Indianapolis, Indiana. [5]Massachusetts General Hospital, Boston, Massachusetts.

Note: Supplementary data for this article are available at Cancer Discovery Online (http://cancerdiscovery.aacrjournals.org/).

Presented in part at meetings of the American Society of Clinical Oncology 2013 and 2014, the American Association for Cancer Research 2014, and the San Antonio Breast Cancer Symposium 2014.

Current address for J.F. Hilton: University of Ottawa, Ottawa, Ontario, Canada.

Corresponding Authors: Amita Patnaik, South Texas Accelerated Research Therapeutics, 4383 Medical Drive, San Antonio, TX 78229. Phone: 210-593-5250; Fax: 210-615-1121; E-mail: amita.patnaik@start.stoh.com; and Geoffrey Shapiro, Early Drug Development Center, Department of Medical Oncology, Dana-Farber Cancer Institute, Mayer 446, 450 Brookline Avenue, Boston, MA 02215. Phone: 617-632-4942; Fax: 617-632-1977; E-mail: geoffrey_shapiro@dfci.harvard.edu

doi: 10.1158/2159-8290.CD-16-0095

INTRODUCTION

Cyclin-dependent kinases (CDK) 4 and 6 interact with D-type cyclins to phosphorylate the retinoblastoma (RB) tumor suppressor protein and promote G_1 to S phase cell-cycle progression (1). The activity of these kinases is regulated by the phosphorylation, ubiquitination, and binding of endogenous cellular inhibitors from the INK4 family (2–5). The INK4–CDK4/CDK6–cyclin D axis is often disrupted in cancer by both genetic and epigenetic mechanisms, resulting in increased kinase activity (6–8). In addition, excessive CDK4 or CDK6 activity may suppress senescence and directly contribute to both initiation and maintenance of the transformed state (9–15). Ectopic expression of INK4-inhibitory proteins in cancer cells reverses these tumorigenic effects, indicating the potential of CDK4 and CDK6 as antineoplastic drug targets (16). Furthermore, mouse models lacking D-type cyclins or CDK4 or CDK6 demonstrate context-specific roles for these proteins in proliferation that is restricted by cell type, suggesting a therapeutic window for inhibition of CDK4 and CDK6 as an anticancer strategy (17–20).

Abemaciclib (LY2835219) is a small-molecule inhibitor of CDK4 and CDK6 that is structurally distinct from other dual inhibitors (such as palbociclib and ribociclib) and notably exhibits greater selectivity for CDK4 compared with CDK6 (21). Consistent with its activity against CDK4 and CDK6, abemaciclib inhibits RB phosphorylation and leads to G_1 arrest in RB-proficient cell lines (21). In a colorectal cancer xenograft model used to develop an integrated pharmacokinetic/pharmacodynamic model, abemaciclib can be dosed orally on a continuous schedule to achieve sustained target inhibition and demonstrates not only durable cell-cycle inhibition but also single-agent antitumor activity (21, 22). Tumor growth inhibition is observed in multiple other human cancer xenograft models, including those derived from non–small cell lung cancer (NSCLC), melanoma, glioblastoma, and mantle cell lymphoma (21–23). Abemaciclib distributes across the blood–brain barrier and prolongs survival in an intracranial glioblastoma xenograft model (24), suggesting potential efficacy against primary and metastatic tumors involving the central nervous system.

Based on preclinical investigations, we conducted a multicenter study including phase I dose escalation and tumor-specific cohorts. The primary objective was to evaluate safety and tolerability of abemaciclib when administered orally on a continuous schedule to patients with advanced cancer. Secondary objectives were to determine pharmacokinetics, evaluate biomarkers, document antitumor activity, and establish a recommended dose range for patients with cancer.

RESULTS

Enrollment

A total of 225 patients with advanced cancer were enrolled between December 28, 2009, and April 28, 2014. Thirty-three patients were enrolled in dose escalation (Supplementary Table S1) and 192 patients in tumor-specific cohorts for breast cancer ($n = 47$, single-agent therapy with abemaciclib), NSCLC ($n = 68$), glioblastoma ($n = 17$), melanoma ($n = 26$), colorectal cancer ($n = 15$), and hormone receptor (HR)–positive breast cancer ($n = 19$, combination therapy with abemaciclib + fulvestrant). Baseline patient and disease characteristics are summarized by cohort and in aggregate for the tumor-specific cohorts in Supplementary Table S2. Notably, most patients had ≥2 metastatic sites and had received multiple prior systemic therapies for advanced cancer.

Dose Escalation

During dose escalation, both once-daily ($n = 13$) and twice-daily ($n = 20$) schedules were investigated. On the once-daily (Q24H) schedule, sequential cohorts of patients received abemaciclib at dose levels of 50 mg ($n = 4$), 100 mg ($n = 3$), 150 mg ($n = 3$), or 225 mg ($n = 3$). Dose-limiting toxicity (DLT) was not observed, and the maximum tolerated dose (MTD) was not reached. On the twice-daily (Q12H) schedule, sequential cohorts of patients received abemaciclib at dose levels of 75 mg ($n = 3$), 100 mg ($n = 4$), 150 mg ($n = 3$), 200 mg ($n = 7$), and 275 mg ($n = 3$). Febrile neutropenia was not observed on either schedule. At 200 mg Q12H, 1 of the 7 patients experienced DLT of grade 3 fatigue. At 275 mg Q12H, 2 of the 3 patients experienced DLT of grade 3 fatigue. Therefore, the MTD for the twice-daily schedule was established at 200 mg Q12H. Both the MTD and 150 mg Q12H were further investigated in the tumor-specific cohorts.

Safety

In the single-agent tumor-specific cohorts ($n = 173$), the most common (>10%) treatment-emergent adverse events (TEAE) possibly related to abemaciclib involved fatigue and the gastrointestinal (diarrhea, nausea, vomiting, anorexia, and weight loss), renal (increased creatinine), or hematopoietic (leukopenia, neutropenia, thrombocytopenia, and anemia) systems (Table 1). These events occurred early, within 1 to 2 weeks of initiating treatment, and were reversible. There were no study-related deaths and only 2 grade 4 events (both neutropenia). Among the 173 patients, febrile neutropenia was observed in 1 patient with breast cancer who received abemaciclib at a dose of 150 mg Q12H. In the tumor-specific cohorts, grade 3 events involving the gastrointestinal and hematopoietic systems occurred in ≤5% and ≤10% of patients, respectively; grade 3 events involving the renal system were not observed, with grade 1 and 2 events occurring in 7% and 4% of patients, respectively. Due to the incidence of grade 1 and 2 diarrhea at 200 mg Q12H, the alternate starting dose of 150 mg Q12H was also explored. Among the 173 patients, dose reductions were required for 17 of 81 patients (21%) receiving a dose of 150 mg Q12H and 40 of 92 patients (43%) receiving a dose of 200 mg Q12H.

For patients with HR-positive breast cancer receiving combination therapy with abemaciclib plus fulvestrant ($n = 19$), the most common possibly related TEAEs were similar to those observed in the single-agent cohorts (Supplementary Table S3). There were no study-related deaths and no grade 4 events. Although grade 1 or 2 diarrhea was common and grade 3 diarrhea occurred in 1 patient (5%), no patients discontinued due to diarrhea. Grade 3 neutropenia occurred in 6 patients (32%); however, febrile neutropenia was not

Table 1. Possibly related treatment-emergent adverse events (>10% all grades) for tumor-specific cohorts

TEAE	Grade 1	Grade 2	Grade 3	Grade 4	All grades[a] ($N = 173$)[b]
Diarrhea	75 (43%)	25 (15%)	9 (5%)	0	109 (63%)
Nausea	59 (34%)	15 (9%)	4 (2%)	0	78 (45%)
Fatigue	38 (22%)	27 (16%)	5 (3%)	0	70 (41%)
Vomiting	31 (18%)	10 (6%)	2 (1%)	0	43 (25%)
Leukopenia	9 (5%)	17 (10%)	17 (10%)	0	43 (25%)
Thrombocytopenia	21 (12%)	7 (4%)	12 (7%)	0	40 (23%)
Neutropenia	6 (4%)	15 (9%)	16 (9%)	2 (1%)	39 (23%)
Anemia	13 (8%)	14 (8%)	7 (4%)	0	34 (20%)
Anorexia	22 (13%)	8 (5%)	0	0	30 (17%)
Increased creatinine[c]	12 (7%)	7 (4%)	0	0	19 (11%)
Weight loss	14 (8%)	4 (2%)	0	0	18 (10%)

NOTE: Data are represented as *n* (%).
[a]No grade 5 events were reported.
[b]Includes all tumor-specific cohorts receiving single-agent abemaciclib for NSCLC, glioblastoma, breast cancer, melanoma, or colorectal cancer.
[c]Abemaciclib inhibits renal transporters that mediate tubular secretion of creatinine, so serum creatinine may not accurately reflect renal function in patients receiving abemaciclib.

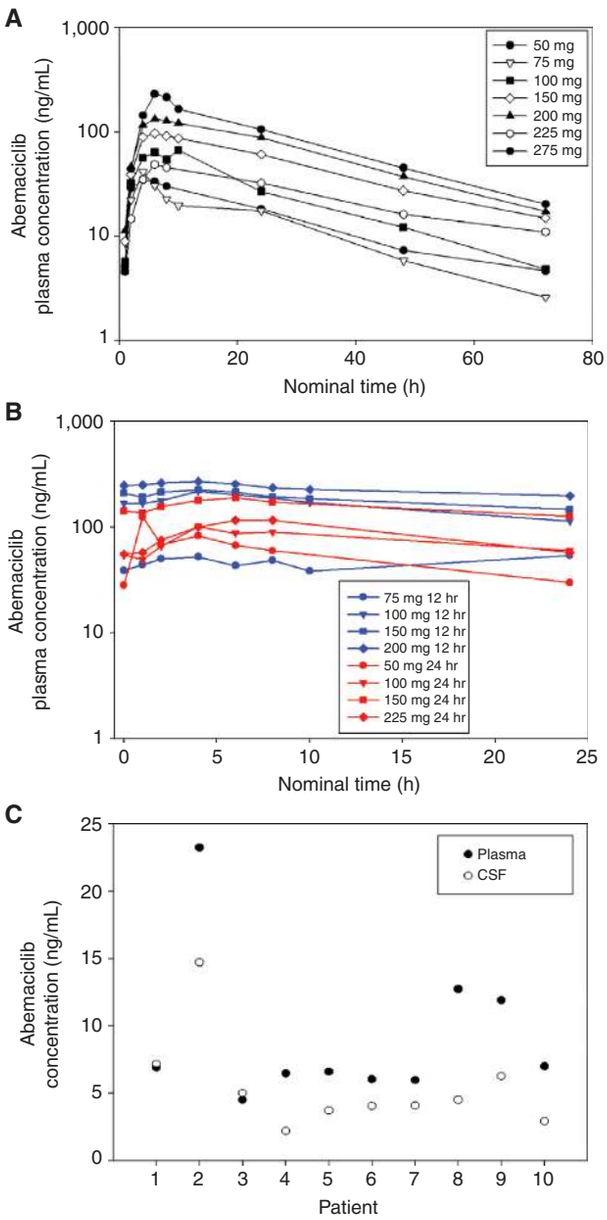

Figure 1. Concentrations of abemaciclib in plasma and cerebrospinal fluid (CSF). Geometric mean time course of abemaciclib plasma concentration (**A**) after single oral dose of abemaciclib ranging from 50 to 275 mg and (**B**) at steady state on once-daily (Q24H) and twice-daily (Q12H) schedules. Observations below the limit of quantitation of the assay were excluded from the analysis. **C,** paired plasma and cerebrospinal fluid concentrations of abemaciclib at steady state.

observed. In combination with fulvestrant, the MTD for abemaciclib was also 200 mg Q12H.

Overall, febrile neutropenia was rare and occurred in only 1 of the 225 patients (0.4%) treated in this study.

Pharmacokinetics

Abemaciclib plasma concentrations increased with dose following a single dose between 50 and 275 mg (Fig. 1A) and at steady state after multiple doses between 50 and 225 mg Q24H or 75 and 200 mg Q12H (Fig. 1B). Relevant pharmacokinetic parameters are summarized in Supplementary Tables S4 and S5. The time course was characterized by a slow absorption phase with a median time from oral dose to maximum plasma concentration (t_{max}) ranging from 4 to 6 hours. Abemaciclib was extensively cleared and distributed. The mean terminal elimination half-life ($t_{1/2}$) ranged from 17.4 to 38.1 hours with no apparent dose-dependent change in clearance. After multiple doses, the mean area under the plasma concentration–time curve over 24 hours at steady state ($AUC_{0\text{-}24,ss}$) reached 4,280 and 5,520 ng-h/mL for 150 mg and 200 mg Q12H, respectively. The mean maximum plasma concentration at steady state ($C_{max,ss}$) reached 249 ng/mL and 298 ng/mL for 150 mg and 200 mg Q12H, respectively.

Both cerebrospinal fluid and unbound plasma concentrations of abemaciclib were obtained on day 15 for 10 patients (Fig. 1C). Cerebrospinal fluid samples were collected for logistical reasons at variable time points (2–8 hours postdose), whereas plasma samples were obtained at a time point (4 hours postdose) approximating mean maximum plasma concentration (C_{max}). Notably, abemaciclib concentrations in the cerebrospinal fluid (range, 2.2–14.7 nmol/L) exceeded the dissociation constant (Ki = 0.6 nmol/L) for the CDK4/cyclin D1 complex and approached unbound plasma concentrations for all these patients.

Pharmacodynamics

In both the dose-escalation and tumor-specific cohorts, phosphorylated RB (pRB) and topoisomerase II alpha (TopoIIα, specific for S phase) were evaluated in epidermal keratinocytes (a proliferative cell population) as integrated pharmacodynamic biomarkers to monitor CDK4/6 inhibition and cell-cycle progression, respectively. Evidence of target engagement, as exemplified by reduced pRB, was observed postdose at steady state on both schedules; however, Q12H dosing was selected for the tumor-specific cohorts to achieve more sustained pharmacodynamic inhibition over the dosing interval. At doses of both 150 mg and 200 mg Q12H, pRB (Fig. 2A; $P < 0.0001$) and TopoIIα expression (Fig. 2B; $P < 0.0001$) was reduced following treatment with abemaciclib. At steady state, reductions in these parameters were comparable whether assessed predose or postdose, indicating sustained CDK inhibition over the dosing interval. The magnitude of pharmacodynamic effect was comparable for 150 mg and 200 mg Q12H across both biomarkers, thereby identifying an oral dose range associated with consistent *in vivo* target inhibition. Importantly, similar pharmacodynamic effects were also observed for pRB (Fig. 2C) and TopoIIα (Fig. 2D) in fresh tumor biopsies collected whenever clinically feasible from patients receiving oral abemaciclib.

To test the hypothesis that a threshold pharmacodynamic effect predicts for disease control, we analyzed maximal percent change in tumor size as a function of percent change in pRB in skin for patients with HR-positive breast cancer in the single-agent cohort (Fig. 2E). This analysis revealed that a decrease in pRB ≥60% separated most patients with stable disease or response from those with progressive disease ($P < 0.0001$) and defined a threshold pharmacodynamic effect that in the absence of biological modifiers involved in

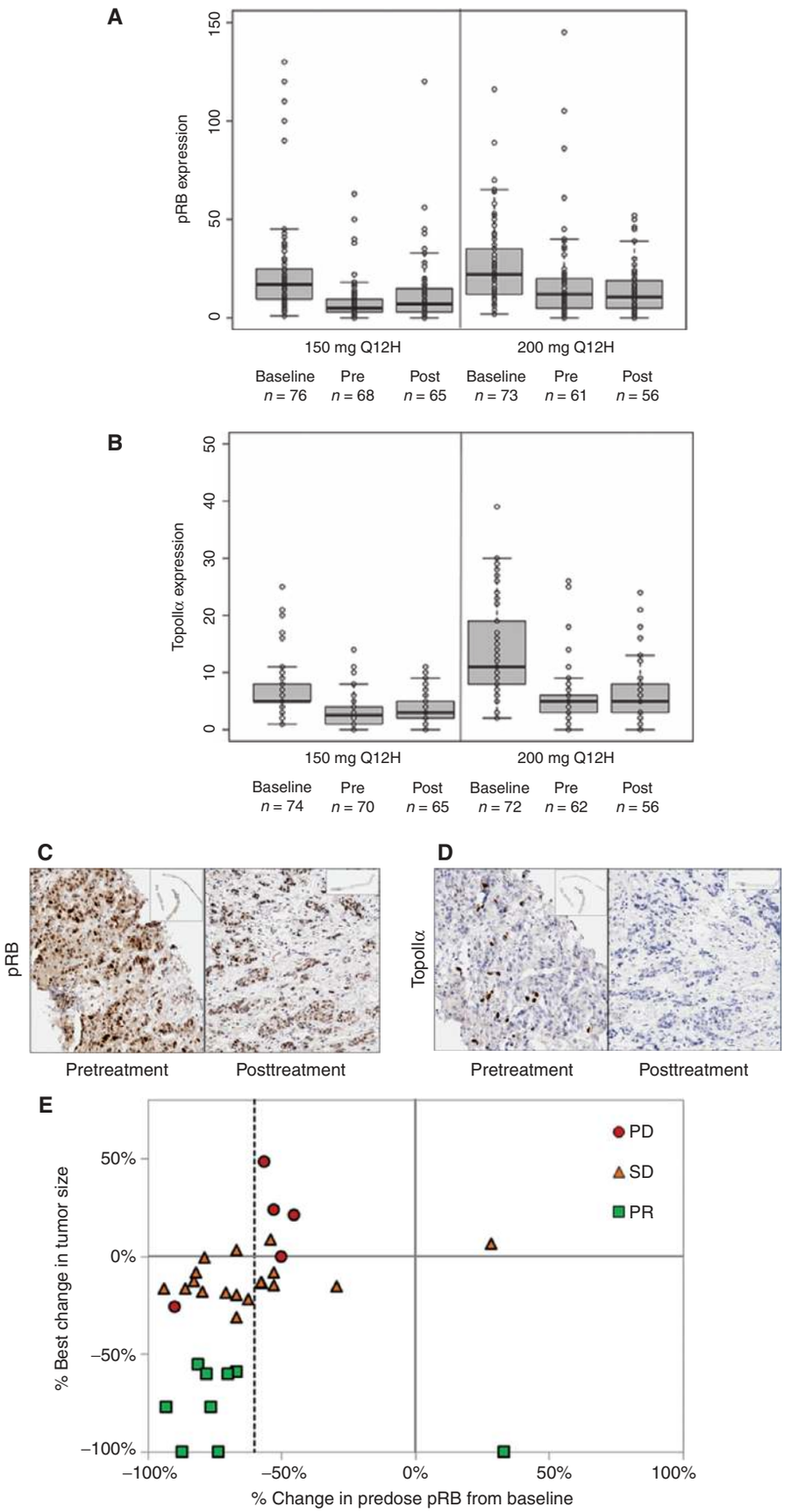

Figure 2. Pharmacodynamic inhibition of phosphorylated retinoblastoma protein (pRB) and topoisomerase IIα (TopoIIα) in skin and tumor biopsies. Serial skin biopsies were collected at baseline, predose at steady state, and postdose at steady state for patients who received abemaciclib at 150 mg or 200 mg Q12H. Expression of pRB (**A**) and TopoIIα (**B**) decreased postdose and remained suppressed predose, indicating sustained pharmacodynamic effect over the 12-hour dosing interval. The magnitude of pharmacodynamic inhibition was similar for the 150-mg and 200-mg dose groups. Serial tumor biopsies were collected pretreatment and posttreatment to evaluate intratumoral expression of pRB and TopoIIα for a patient with breast cancer who received abemaciclib (150 mg Q12H) for 16 cycles without radiographic progression (**C** and **D,** respectively). Pharmacodynamic effect was observed for both biomarkers and this patient achieved a partial response. **E,** analysis of maximal percent change in tumor size as a function of percentage change in pRB in skin for patients with HR-positive breast cancer receiving abemaciclib in the single-agent cohort. A decrease in pRB levels ≥60% compared with baseline (indicated by vertical dotted line) separated most patients with stable disease or response from those with progressive disease. *n*, number of patients with evaluable sample for marker of interest; PD, progressive disease; PR, partial response; Pre, predose; Post, postdose; Q12H, every 12 hours (twice daily); Q24H, every 24 hours (once daily); SD, stable disease.

resistance may be associated with optimal clinical activity. Within this cohort, 1 patient with an increase in pRB achieved a partial response and 1 patient with a decrease in pRB ≥60% experienced progressive disease as best response; this latter patient had an HR-positive, HER2-negative breast carcinoma characterized by *CCND1* amplification, *CDKN2A* mutation, and *TP53* mutation.

Breast Cancer

Because CDK4 activity is particularly important to the proliferation of luminal HR-positive tumors (25, 26), we tested the activity of abemaciclib in relevant HR-positive breast cancer models. In a representative estrogen receptor (ER)–positive and HER2-negative human breast cancer xenograft (T47D), abemaciclib demonstrates antitumor activity as a monotherapy (Fig. 3A). Consistent with these preclinical results, radiographic responses were observed among patients with previously treated HR-positive breast cancer receiving abemaciclib as a single agent. Importantly, these responses were not limited to patients with HER2-negative disease and also included those with HR-positive, HER2-positive breast cancer (Fig. 3B).

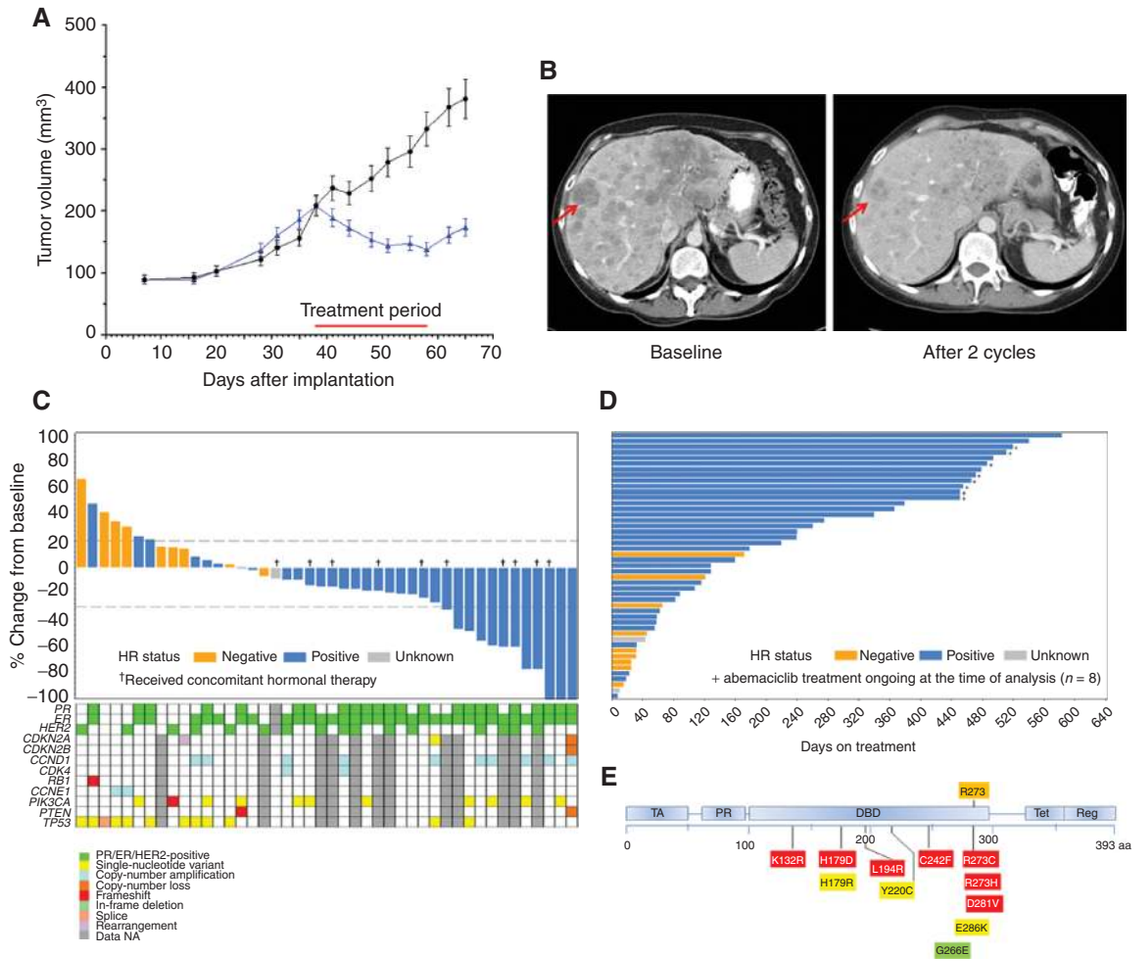

Figure 3. Breast cancer. **A,** antitumor activity of abemaciclib in a human xenograft model (T47D) of ER-positive, HER2-negative breast cancer. Athymic nude mice implanted with human xenograft tumors (T47D) were treated orally once daily for 21 days with vehicle [1% hydroxyethyl cellulose (HEC) shown in black], or abemaciclib mesylate (75 mg/kg/d; shown in blue). The horizontal red bar below the *x*-axis indicates the treatment period. **B,** patient with HR-positive, HER2-positive breast cancer and extensive hepatic metastases who received oral abemaciclib (200 mg every 12 hours). She had recurrence after adjuvant chemotherapy plus endocrine therapy and had received treatment for metastatic disease with vinorelbine, trastuzumab, gemcitabine, lapatinib plus capecitabine, liposomal doxorubicin, and eribulin. **C,** waterfall plot of maximal percentage change in tumor size for the cohort of patients receiving abemaciclib for advanced breast cancer. Patients with at least 1 posttreatment radiographic assessment were included. Positive values indicate tumor growth, and negative values indicate tumor reduction. The upper and lower dashed lines depict thresholds defined in RECIST v1.1 for progressive disease and partial response, respectively. Genetic features (as determined by next-generation sequencing) and clinical markers (as reported by investigators) for each patient are summarized in the accompanying heat map. PR, progesterone receptor; NA, not available. **D,** duration of therapy with abemaciclib for patients with breast cancer. **E,** mapping of mutations in the tumor suppressor protein p53 identified among the patients with breast cancer. All mutations mapped to the DNA-binding domain of p53 (protein domain map modified from ref. 47). Mutations identified in this study are indicated below the protein domain map and included R273 mutations (location indicated in orange above the protein domain map), which alter contact of p53 with DNA. DBD, DNA-binding domain; PR, proline-rich domain; Reg, carboxy-terminal regulatory domain; TA, transactivation domain; TET, tetramerization domain.

Table 2. Efficacy for single-agent breast cancer cohort, overall and by HR and HER2 status

Endpoint	Breast cancer overall[a] (*N* = 47)	HR-positive (*N* = 36)	HR-negative (*N* = 9)	HR-positive, HER2-positive (*N* = 11)	HR-positive, HER2-negative (*N* = 25)
Best overall response					
CR	0	0	0	0	0
PR	11 (23%)[b]	11 (31%)	0	4 (36%)	7 (28%)
SD	22 (47%)	18 (50%)	3 (33%)	7 (64%)	11 (44%)
≥24 weeks	12 (26%)	11 (31%)	1 (11%)	2 (18%)	9 (36%)
<24 weeks	10 (21%)	7 (19%)	2 (22%)	5 (45%)	2 (8%)
Progressive disease	11 (23%)	5 (14%)	6 (67%)	0	5 (20%)
Not evaluable	3 (6%)	2 (6%)	0	0	2 (8%)
Response rate (CR + PR), (95% CI)	23% (12.3–38.0)	31% (16.3–48.1)	0% (0–33·6)	36% (10.9–69.2)	28% (12.1–49.4)
Clinical benefit rate (CR + PR + SD ≥ 24 weeks), (95% CI)	49% (34.1–63.9)	61.1% (43.5–76.9)	11.1% (0.3–48.2)	54.5% (23.4–83.3)	64% (42.5–82.0)
Disease control rate (CR + PR + SD), (95% CI)	70% (55.1–82.7)	81% (64.0–91.8)	33% (7.5–70.1)	100% (71.5–100.0)	72% (50.6–87.9)
Median duration of response,[c] months	13.4 (9.0–13.4) (11 patients)	13.4 (3.7–13.4)	NA[d]	4.6, 10.0, 9.2, 5.3 (4 patients)	13.4 (3.7–13.4)
Median PFS (95% CI), months	5.8 (2.9–10.9)	8.8 (4.2–16.0)	1.1 (0.6–4.0)	7.2 (2.8–12.0)	8.8 (2.9–18.0)

NOTE: Data are represented as *n* (%), unless otherwise specified.
Abbreviations: CI, confidence interval; NA, not available.
[a]Two patients had unknown HR status.
[b]All 11 patients with breast cancer who had a partial response were HR-positive.
[c]Median duration of response is reported if ≥5 patients had a response in each category. If <5 patients had a response, individual values are presented.
[d]Duration of response was not available for patients with HR-negative breast cancer as none of these patients had a partial response.

To extend these findings, we characterized the clinical activity of abemaciclib in a cohort of 47 patients with advanced breast cancer who had received a median of 7 (range, 2–16) prior systemic therapies. Ten of the 47 patients who had progression on prior endocrine therapy continued endocrine therapy with the addition of abemaciclib. The disease control rate [complete response (CR) + partial response (PR) + stable disease (SD)] was higher for HR-positive tumors (29 of 36 patients, 81%) versus HR-negative tumors (3 of 9 patients, 33%), and radiographic responses occurred exclusively in the HR-positive population (Table 2). Among the 36 patients with HR-positive breast cancer, 11 (31%) achieved partial response (4 of whom had continued prior endocrine therapy) and 18 (50%) achieved stable disease, including 11 (31%) with stable disease for ≥24 weeks; thus, the clinical benefit rate (CR + PR + SD for ≥24 weeks) was 61%. Of the 11 responses in the HR-positive population, 7 were observed among 25 patients (28%) with HER2-negative disease and 4 occurred among 11 patients (36%) with HER2-positive disease. For the overall HR-positive population, median duration of response was 13.4 months (95% CI, 3.7–13.4) and median progression-free survival (PFS) was 8.8 months (95% CI, 4.2–16.0). Change in tumor size at best response, along with genetic features and clinical markers, is depicted graphically for the single-agent breast cancer cohort (Fig. 3C) and highlights the activity of abemaciclib in HR-positive breast cancer. Duration of therapy is also summarized for these patients (Fig. 3D) and is notable for the durability of disease control in the absence of radiographic progression. Nonresponding breast tumors were more likely to harbor *TP53* mutations, with all mutations observed occurring in the region encoding the p53 DNA-binding domain (Fig. 3E). Importantly, abemaciclib demonstrated clinical activity in HR-positive breast cancers with or without *PIK3CA* mutations.

To evaluate the potential for combining abemaciclib with endocrine agents for the treatment of HR-positive breast cancer, we investigated combination therapy with abemaciclib plus fulvestrant, an antiestrogen that induces selective degradation of the estrogen receptor. The 19 patients in the combination cohort for HR-positive breast cancer had received a median of 4 (range, 1–11) prior systemic therapies, and all patients had received prior endocrine therapy. Both abemaciclib (200 mg Q12H) and fulvestrant (500 mg once monthly) were given at MTD. Partial responses were observed in 4 patients, resulting in a response rate of 21% (4 of 19 patients) for all patients (measurable or nonmeasurable disease) and a response rate of 36% (4 of 11 patients) for those patients with measurable disease. Although the disease control rate (15 of 19 patients, 79%) and clinical benefit rate (12 of

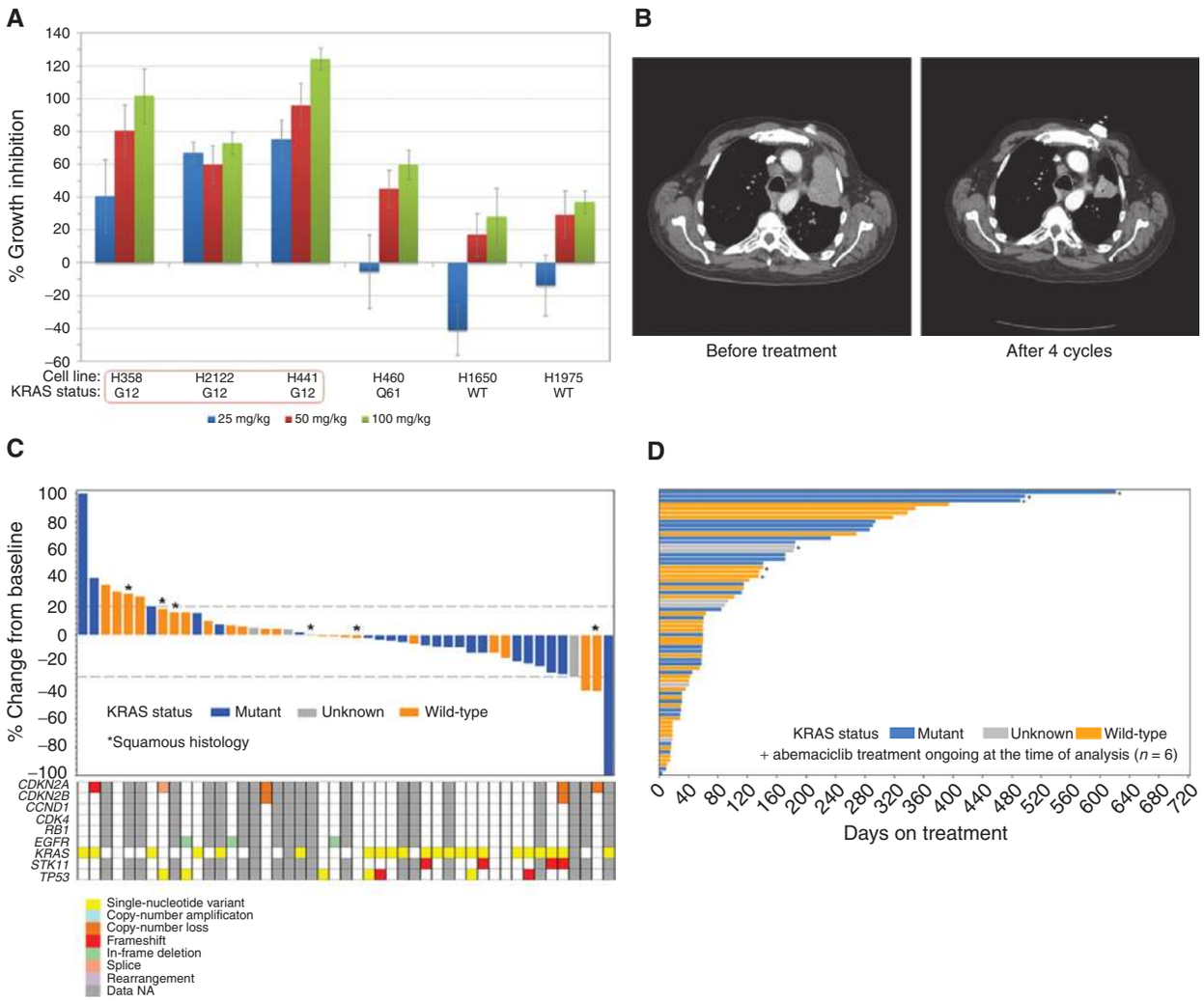

Figure 4. NSCLC. **A,** antitumor activity of abemaciclib in 4 *KRAS*-mutant (NCI-H358, NCI-H2122, NCI-H441, NCI-H460) and 2 *KRAS* wild-type (WT; NCI-H1650, NCI-H1975) human xenograft models of NSCLC. Athymic nude mice implanted with human NSCLC xenograft tumors were treated orally once daily for 21 days with vehicle (1% HEC) or abemaciclib mesylate (25, 50, or 100 mg/kg/d). Tumor growth inhibition compared with the vehicle control group was determined after 21 days of oral dosing with abemaciclib mesylate. **B,** patient with *KRAS*-mutant NSCLC and symptomatic left upper lobe primary tumor who received abemaciclib (200 mg orally Q12H). He had previously received first-line treatment with paclitaxel plus carboplatin and second-line treatment with pemetrexed. **C,** waterfall plot of maximal percentage change in tumor size for the cohort of patients receiving abemaciclib for advanced NSCLC. Patients with at least 1 posttreatment radiographic assessment were included. Positive values indicate tumor growth and negative values indicate tumor reduction. The upper and lower dashed lines depict thresholds defined in RECIST v1.1 for progressive disease and partial response, respectively. Genetic features (as determined by next-generation sequencing) for each patient are summarized in the accompanying heat map. NA, not available. **D,** duration of therapy with abemaciclib for patients with NSCLC.

19 patients, 63%) were comparable to those among HR-positive patients in the single-agent cohort, several important factors (such as differences in eligibility criteria, nonrandomized design, and sample sizes for these cohorts) limit the ability to compare efficacy for abemaciclib plus fulvestrant versus abemaciclib alone.

NSCLC

In a genetically engineered mouse model of *KRAS*-mutant NSCLC, genetic ablation of CDK4 induces senescence and prevents tumor progression (14). In complementary pharmacologic experiments, we tested whether abemaciclib preferentially inhibits growth of *KRAS*-mutant versus wild-type NSCLC xenografts. Among 6 human xenograft models of NSCLC, tumors with *KRAS* mutation were more sensitive to abemaciclib than *KRAS* wild-type tumors (Fig. 4A). Consistent with these preclinical results, evidence of single-agent antitumor activity was observed among patients with previously treated *KRAS*-mutant NSCLC (Fig. 4B).

To extend these findings, we evaluated the clinical activity of abemaciclib in a cohort of 68 patients with NSCLC who had received a median of 4 (range, 1–10) prior systemic

therapies, including 29 patients who had tumors harboring *KRAS* mutations. For the overall population (68 patients), the disease control rate (CR + PR + SD) was 49% (33 of 68 patients). Thirty-one of 68 patients (46%) achieved stable disease, including 15 patients (22%) with stable disease lasting for ≥24 weeks. The 6-month PFS rate was 26% (95% CI, 16%–38%), with 4 patients receiving single-agent abemaciclib without progression for ≥12 months (Supplementary Table S6). Partial response was achieved for 1 patient with *KRAS*-mutant NSCLC and for 1 patient with *KRAS* wild-type squamous NSCLC bearing copy-number loss of *CDKN2A*.

KRAS mutations most often involved codon 12 or 13, but tumors with less-frequent mutations (Q61H, A146V) were also detected and associated with decreases in tumor size following single-agent treatment with abemaciclib (27). The disease control rate for the *KRAS*-mutant population was 55% (16 of 29 patients), whereas that for the *KRAS* wild-type population was 39% (13 of 33 patients); moreover, stable disease lasting ≥24 weeks was achieved for 9 of the 29 patients (31%) with *KRAS*-mutant disease compared with 4 of 33 patients (12%) with *KRAS* wild-type disease (Supplementary Table S6). Finally, median PFS was 2.8 months (95% CI, 1.8–5.6) and 1.9 months (95% CI, 1.4–3.7) for the *KRAS*-mutant and *KRAS* wild-type populations, respectively.

Change in tumor size at best response, along with genetic features, is depicted graphically for the NSCLC cohort (Fig. 4C) and highlights the sensitivity of *KRAS*-mutant tumors. Decrease in tumor size was more common for *KRAS*-mutant disease, whereas increase in tumor size was more frequent for *KRAS* wild-type disease. For molecular subsets of *KRAS*-mutant adenocarcinoma (28), a decrease in tumor size was observed among evaluable patients for 4 of 4 *KRAS*-mutant tumors with concomitant *TP53* alterations (KP subgroup) and 4 of 4 *KRAS*-mutant tumors with concomitant *STK11/LKB1* alterations (KL subgroup). Duration of therapy is also summarized for patients in the NSCLC cohort (Fig. 4D). Notably, 3 of the 4 patients who received abemaciclib in the absence of radiographic progression for ≥12 months had tumors harboring *KRAS* mutation.

Other Tumors

Ovarian cancer frequently harbors genetic or epigenetic alterations that aberrantly activate CDK4 or CDK6 (29). We therefore tested whether abemaciclib could prolong survival in a human xenograft model (SKOV3-Luciferase) that recapitulates the characteristic intraperitoneal dissemination of ovarian cancer in patients (Fig. 5A). In this orthotopic model, oral abemaciclib induced a dose-dependent prolongation of survival with no deaths at the highest dose level. Consistent with these preclinical results, we observed 2 patients with ovarian cancer who achieved stable disease based on RECIST version 1.1 for 4 and 6 cycles (abemaciclib 225 mg Q24H and 200 mg Q12H, respectively) and one patient with ovarian cancer who achieved a rapid and durable CA-125 response based on criteria of the Gynecological Cancer Intergroup (30) and received single-agent therapy (abemaciclib 150 mg Q24H) for 24 cycles without radiographic progression (Fig. 5B).

The clinical activity of abemaciclib was also investigated in tumor-specific cohorts for cancers characterized by relevant pathway alterations, including glioblastoma, colorectal cancer, and melanoma (Fig. 5C and Supplementary Table S7; refs. 31–33). Consistent with detection of abemaciclib in cerebrospinal fluid from patients at concentrations associated with target inhibition (CDK4/cyclin D1 Ki = 0.6 nmol/L), 3 patients with glioblastoma achieved stable disease, and 2 of these patients have continued to receive ongoing treatment without progression for 19 and 23 cycles, respectively. Both glioblastomas with durable disease control on single-agent abemaciclib had *TP53* mutations, and one also had a frameshift mutation in the gene encoding the epidermal growth factor receptor (EGFR). These results are compatible with distribution of abemaciclib to the central nervous system. In the colorectal cancer cohort, 2 patients achieved stable disease, including 1 patient with a tumor that harbored both *KRAS* and *TP53* mutations. In the melanoma cohort, 1 patient achieved RECIST partial response and 6 patients achieved stable disease, for a disease control rate of 27% (7 of 26 patients). Among the 16 patients with melanoma and available next-generation sequencing results, tumors harboring $BRAF^{V600E/K}$ mutations were relatively uncommon (2 patients) with corresponding enrichment for *NRAS* mutations (6 patients). Notably, the patient with metastatic melanoma who achieved a partial response had a tumor with molecular alterations (*NRAS* mutation and copy-number loss at the *INK4* locus) that induced aberrant kinase activity of CDK4 and CDK6.

DISCUSSION

This report encompasses the first-in-human experience with abemaciclib, a dual inhibitor of CDK4 and CDK6 with greater selectivity for CDK4. Clinical development of this drug has utilized systematic integration of pharmacokinetic parameters with pharmacodynamic biomarkers across preclinical (22) and clinical studies in order to optimize dose, schedule, and antitumor efficacy. The combination of traditional phase I and II design elements, as well as the incorporation of biomarkers and genomic profiling, has allowed refinement of dosing to achieve sustained target inhibition, detection of efficacy signals in multiple tumor types, generation of hypotheses for tailoring abemaciclib therapy to patient populations most likely to respond, and early initiation of confirmatory phase III studies.

We have established that abemaciclib can be dosed safely on a continuous schedule. Among treatment-emergent adverse events, fatigue was dose limiting, but gastrointestinal, renal, and hematopoietic effects were also observed. Diarrhea was manageable with antidiarrheal agents or dose reduction and did not result in patient discontinuation. Because abemaciclib inhibits renal efflux transporters [multidrug and toxin extrusion (MATE) 1 and 2-K] that mediate active secretion of creatinine from the proximal tubule, increases in serum creatinine during therapy with abemaciclib may not accurately reflect renal function, and measures of glomerular filtration rate that are independent of active tubular secretion via renal efflux transporters (such as cystatin C) may yield a more accurate estimate of renal function than serum creatinine for patients receiving the drug. Previous reports have identified neutropenia as an adverse event associated with dual inhibition of CDK4 and CDK6 (34–39). However, abemaciclib given

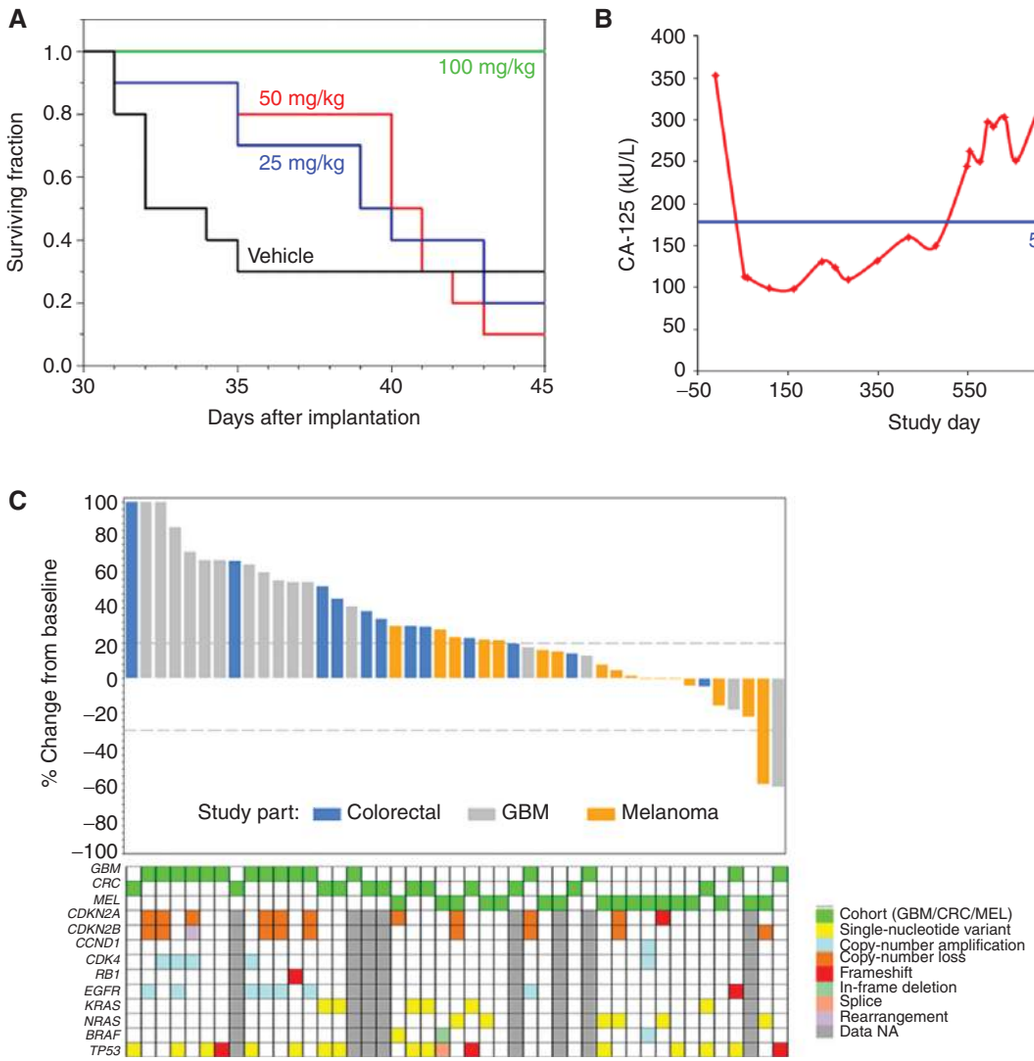

Figure 5. Other tumors. **A,** abemaciclib prolongs overall survival in an intraperitoneal model of ovarian cancer. Athymic nude mice implanted with human ovarian xenograft tumors (SKOV3-Luciferase) were treated once daily (beginning on day 10 after implantation) for 21 days with vehicle (1% HEC) or abemaciclib mesylate (25, 50, or 100 mg/kg/d). Mean survival ± SEM (in days) following the 21-day dosing interval was 36.2 ± 2.0 (vehicle control), 39.5 ± 1.5 (25 mg/kg/d), 39.8 ± 1.3 (50 mg/kg/d), and >45 (100 mg/kg/d), respectively. No deaths were observed in the group treated with abemaciclib mesylate at 100 mg/kg. Survival was significantly different from the vehicle control group compared with the groups treated with abemaciclib mesylate at 50 mg/kg/d ($P = 0.0462$) and 100 mg/kg/d ($P < 0.0001$). **B,** abemaciclib (150 mg once daily) induced durable CA-125 response for a patient with advanced ovarian cancer. She had recurrence after first-line treatment with paclitaxel plus carboplatin, and had received second-line treatment with paclitaxel plus carboplatin, and third-line treatment with topotecan. **C,** waterfall plot of maximal percent change in tumor size for the cohorts of patients receiving abemaciclib for advanced colorectal cancer, glioblastoma, or melanoma. Patients with at least 1 posttreatment radiographic assessment were included. Positive values indicate tumor growth, and negative values indicate tumor reduction. The upper and lower dashed lines depict thresholds defined in RECIST v1.1 for progressive disease and partial response, respectively. Genetic features (as determined by next-generation sequencing) are summarized in the accompanying heat map. CRC, colorectal cancer; GBM, glioblastoma; MEL, melanoma; NA, not available.

as a single agent on a continuous schedule in the tumor-specific cohorts was associated with an acceptable incidence of investigator-reported grade 3 (9%, 16 of 173 patients) or grade 4 (1%, 2 of 173 patients) neutropenia. Febrile neutropenia was rare, occurring in only 1 patient over the entire study. This sparing of the hematopoietic system, which obviates the need for an intermittent dosing schedule (as required for palbociclib and ribociclib) and provides important opportunities for combining abemaciclib with a broad range of targeted or cytotoxic agents, may arise from greater selectivity for CDK4 compared with CDK6, pharmacokinetic considerations associated with Q12H dosing, metabolism to products with minimal hematologic toxicity, or a combination of these factors.

Plasma concentrations for abemaciclib increased with dose, and mean exposures at 150 mg or 200 mg Q12H were associated with evidence of target engagement in both proliferating epidermal keratinocytes and tumor cells. Assessment of direct biochemical inhibition (reduced pRB) and phenotypic G1 arrest (reduced TopoIIα) demonstrated that Q12H dosing achieved sustained pharmacodynamic effects. Consistent with

previous findings in mouse xenograft models (22), a decrease in pRB ≥60% identified a group of patients with HR-positive breast cancer who were likely to achieve stable disease or response. Although pharmacodynamic effects were observed at both dose levels, fewer dose reductions were required among those patients who initiated treatment at 150 mg Q12H. However, the broad dose range associated with clinical efficacy and the presence of interpatient pharmacokinetic variability support the concept that some patients may derive optimal antitumor efficacy from dosing at 200 mg Q12H. Therefore, the recommended starting dose for abemaciclib as a single agent is 200 mg Q12H, with supportive measures or dose reduction if necessary to achieve acceptable tolerability for an individual patient. In certain clinical contexts, however, it may be reasonable to initiate therapy with abemaciclib at 150 mg Q12H to limit toxicity and to consider dose escalation to 200 mg Q12H for an individual patient with acceptable tolerability but suboptimal response. Abemaciclib was also detectable in the cerebrospinal fluid of patients at concentrations approximating those of unbound drug in plasma, and 2 patients with glioblastoma have achieved prolonged PFS. Accordingly, abemaciclib is being investigated in a clinical trial for patients with brain metastases (NCT02308020).

KRAS mutations are found in approximately 30% of lung adenocarcinomas and confer an adverse prognosis compared with *KRAS* wild-type tumors (40). Among the heavily pretreated patients in the NSCLC cohort, responses were uncommon, but the disease control rate was greater in the *KRAS*-mutant population compared with the *KRAS* wild-type population, due in large part to more than a doubling of the number (and also the percentage) of patients with stable disease lasting ≥24 weeks. Moreover, the majority of tumor regressions in the group with stable disease also occurred in *KRAS*-mutant patients. Although outcomes from ongoing clinical trials will be required to confirm whether the presence of *KRAS* mutation identifies a population with NSCLC sensitive to abemaciclib, the results from the current study are consistent with the greater sensitivity of *KRAS*-mutant versus *KRAS* wild-type NSCLC xenografts, as well as the synthetic lethal interaction observed with genetic inactivation of CDK4 in *KRAS*-driven mouse models of lung adenocarcinoma (14). The activity observed in the *KRAS/LKB1* (KL) subset is particularly noteworthy, as this group has recently been associated with aggressive phenotype (41) and was poorly responsive to other therapeutic approaches in preclinical models, including taxane-based chemotherapy and MEK inhibition (42). Collectively, these findings support the investigation of abemaciclib for patients with *KRAS*-mutant NSCLC in an ongoing phase III trial (NCT02152631).

Similar to NSCLC, colorectal cancer frequently harbors *KRAS* mutation. Although stable disease was achieved for some patients with colorectal cancer, durability was relatively short, and progressive disease was typical for most patients. In this regard, it is important to emphasize that synthetic lethality between *KRAS* mutation and CDK4 inhibition may depend upon tumor type and molecular context (14).

For melanoma, abemaciclib as a single agent achieved a disease control rate of 27% and induced a partial response for 1 patient with metastatic melanoma harboring both *NRAS* mutation and copy-number loss at the *INK4* locus. However, the relatively low representation of *BRAF*-mutant disease in the current study may have limited the opportunity to observe maximal clinical activity, as preclinical studies with abemaciclib in models of human melanoma indicate that the drug may have particular clinical application in reversing resistance to selective *BRAF* inhibitors in melanomas characterized by $BRAF^{V600E/K}$ mutations (23).

Preclinical studies in breast cancer models utilizing genetic or pharmacologic ablation of CDK4 activity have predicted the efficacy of CDK4 inhibitors in both HR-positive and HER2-positive disease (11, 26). Clinical investigation with palbociclib as a single agent in patients with HR-positive breast cancer showed an overall response rate (ORR) of 6% (2 of 33 patients), a clinical benefit rate (CBR) of 21% (7 of 33 patients), and a median PFS of 4.5 months (43). Among patients with HR-positive disease enrolled in the breast cancer cohort of the current clinical trial (Fig. 3C and D), abemaciclib therapy demonstrated an ORR of 31% (11 of 36 patients), a CBR of 61% (22 of 36 patients), and a median PFS of 8.8 months. Based on these results, abemaciclib is currently under active clinical investigation for patients with HR-positive advanced breast cancer in a phase II study as a single agent (NCT02102490) and in two phase III studies in combination with either fulvestrant (NCT02107703) or aromatase inhibitors (NCT02246621).

TP53 mutations localized to the region encoding the DNA-binding domain of p53 and were enriched among breast cancers with increase in tumor size at best response. Although it is not yet known whether these mutations confer intrinsic resistance in breast cancer, it is intriguing that p53 plays a role in triggering senescence, which may represent an important mechanism for the antitumor effects of agents that inhibit CDK4 or CDK6 (44).

Although partial responses were observed for HER2-positive or *PIK3CA*-mutated breast cancers in the context of HR-positive disease, further work will be required to define the role for abemaciclib in tumors with these molecular features. To investigate potential therapeutic opportunities, abemaciclib is being studied for patients with breast cancer in combination with both endocrine therapies and agents targeting the HER2 or PI3K–AKT–mTOR pathways (NCT02057133).

In summary, the results of this clinical trial demonstrate the safety and antitumor activity of abemaciclib as a single agent and support its further development both as monotherapy and in rational combinations. Furthermore, these findings validate CDK4 and CDK6 as anticancer drug targets and translate preclinical predictions regarding therapeutic targeting of cell-cycle derangements in cancer into clinical efficacy.

METHODS

Preclinical Studies

All cell lines were authenticated by genetic testing (IDEXX Bioresearch) and were obtained from the centralized cell bank maintained by Eli Lilly and Company. For human xenograft studies, athymic nude mice were implanted with human tumor cells either subcutaneously or directly into the peritoneal cavity. After tumors were established *in vivo*, cohorts of mice were treated orally with either vehicle or abemaciclib mesylate (range, 25–100 mg/kg/d) for a period of approximately 21 days. Tumor measurements were performed quantitatively by physical measurement (subcutaneous models) or noninvasive imaging (intraperitoneal model) at regular intervals. All animal studies were

performed in accordance with American Association for Laboratory Animal Care institutional guidelines, and all protocols were approved by the Eli Lilly and Company Animal Care and Use Committee.

Study Design

Dose escalation was performed using a 3+3 design. Two continuous administration schedules were studied: 50, 100, 150, or 225 mg orally every 24 hours (Q24H) and 75, 100, 150, 200, or 275 mg orally every 12 hours (Q12H). After determination of the single-agent MTD, abemaciclib (150 mg Q12H or 200 mg Q12H) was assessed in tumor-specific cohorts for breast cancer, NSCLC, glioblastoma, melanoma, and colorectal cancer. An additional cohort for HR-positive breast cancer evaluated combination safety for abemaciclib plus fulvestrant. The trial was conducted in accordance with the Declaration of Helsinki and the International Conference on Harmonisation. The protocol was approved by all institutional review boards, and written informed consent was collected from all patients before conducting study procedures. This study is registered with ClinicalTrials.gov (NCT01394016).

Patients

Eligible patients were 18 years or older with advanced cancer, no longer receiving benefit from available standard therapies, with adequate organ function and Eastern Cooperative Oncology Group performance status ≤1 (dose escalation) or ≤2 (tumor-specific cohorts). Measurable disease was required in the single-agent tumor-specific cohorts and was defined by RECIST version 1.1 (45). Prior cancer treatments must have been discontinued 14 or 21 days for nonmyelosuppressive and myelosuppressive therapies, respectively; however, patients in the single-agent breast cancer cohort who had progressed on endocrine therapy were permitted to continue that specific therapy. Patients with disease in the central nervous system were excluded from dose escalation but permitted in tumor-specific cohorts if there was radiographic and clinical stability for at least 14 days.

Procedures

During dose escalation, cohorts of 3 patients were sequentially enrolled at successive dose levels. A single dose of abemaciclib was administered on day −3 for determination of single-dose pharmacokinetics, with continuous dosing beginning on day 1. Adverse events were graded using the Common Terminology Criteria for Adverse Events (CTCAE; Version 4.0). Dose escalation was guided by safety during cycle 1 and informed by pharmacokinetic data.

DLT was defined as the following possibly drug-related events occurring during cycle 1: grade 3 or 4 nonhematologic toxicity (except for nausea, vomiting, diarrhea, or electrolyte disturbance, which were considered dose limiting only if they persisted >2 days despite maximal supportive intervention); grade 4 hematologic toxicity that persisted >5 days; grade 3 or 4 thrombocytopenia with bleeding; and grade 3 or 4 neutropenia with fever. Dose adjustments were required for patients with possibly related grade ≥3 nonhematologic toxicity or grade 4 hematologic toxicity and were permitted for patients with omission of >25% of doses in a single cycle due to tolerability. MTD was defined as the highest dose level at which <33% of patients experienced DLT.

Tumor response was assessed every 2 cycles by investigators, and retrospectively by independent central review for patients with investigator-assessed stable disease or response, using either computed tomography (CT) or MRI scans in accordance with RECIST version 1.1 (45).

Pharmacokinetics

Pharmacokinetic sampling was performed from plasma and, in a subset of patients, from cerebrospinal fluid. Drug concentrations were assayed using a validated method for liquid chromatography with tandem mass spectrometry. For plasma, sampling was performed on day −3 (predose and 1, 2, 4, 6, 8, and 10 hours postdose), day −2 (24 hours postdose), day −1 (48 hours postdose), and day 1 (72 hours postdose), day 15 (predose and 1, 2, and 4 hours postdose), day 22 (predose), and day 28 (predose and 1, 2, 4, 6, 8, 10, and 24 hours postdose). For cerebrospinal fluid, sampling was performed at baseline (day −14 to day −3) and on day 15 (2–8 hours postdose).

Pharmacodynamic and Genomic Analyses

Skin biopsies were performed pretreatment and on day 15 (predose and 4 hours postdose) and analyzed for pRB (Ser780; BD Biosciences #558385) and TopoIIα (Epitomics #1826-1) by immunohistochemistry to quantitate expression by H-score (H-score = weighted sum of % 1+ cells, twice % 2+ cells, and three times % 3+ cells; range, 0–300). Paired tumor biopsies were obtained from selected patients before treatment (between days −14 and −4) and on treatment (between days 8 and 22) during cycle 1. Available archived tumors were subjected to next-generation sequencing using platforms compliant with Clinical Laboratory Improvement Amendments (CLIA).

Sample Size and Statistical Analysis

Although at least 15 patients were to be enrolled in each of the tumor-specific expansions, up to 45 to 60 patients could be enrolled in each tumor-specific expansion. The target sample size of up to 45 to 60 patients was based on differentiating 34.5% to 40% from 5% (uninteresting) ORR in tumors with (marker present) and without (marker absent) a relevant tumor biomarker, respectively (that is, $ORR_{marker\ present}$ = 34.5%–40% and $ORR_{marker\ absent}$ = 5%). Examples of relevant tumor biomarkers included *KRAS* status (mutant versus wild-type; NSCLC) and HR status (positive versus negative; breast cancer). Assuming an equal number of patients having tumors with and without the biomarker, 45 or 60 patients provided approximately 85% power to differentiate 40% or 34.5% from 5% ORR, respectively. To maximize the power to detect the ORR difference between the biomarker groups, enrollment to a tumor-specific expansion could be adjusted to achieve approximately an equal number of patients having tumors with and without the biomarker.

All patients who received at least 1 dose of abemaciclib were included in safety and efficacy analyses. Patient results were summarized by dose level (escalation) or tumor-specific cohort. Pharmacokinetic parameters were computed by standard noncompartmental methods. For analysis of pharmacodynamic response during drug treatment, a paired Wilcoxon test was used to compare the distributions of pRB or TopoIIα expression in skin at baseline versus during treatment (predose or postdose) on day 15. An unpaired Wilcoxon test was used to compare the distributions of maximal percent change in tumor size in subgroups of patients with HR-positive breast cancer with <60% versus ≥60% decrease in pRB expression in skin (predose) on day 15. Median duration of response and median PFS were estimated using the Kaplan–Meier method (46).

Disclosure of Potential Conflicts of Interest

L.S. Rosen reports receiving commercial research support from Eli Lilly and Company. A.W. Tolcher is a board member for Symphogen and a consultant/advisory board member for Arqule, Astex, Bayer Schering Pharma, Bind Therapeutics, Blend, Celator, Dicerma, Janssen, Merus, Nanobiotix, Pharmacyclics, Pierre Fabre, Valent, Heron, Johnson & Johnson, Asana, Akebia, Genmab, AP Pharma, Mersana, Endocyte, Proximagen, Upsher-Smith, Eli Lilly and Company, Idea Pharma, LiquidNet, MedImmune, and Symphogen. L. Gandhi reports receiving a commercial research grant from BMS, and is a consultant/

advisory board member for Genentech/Roche, AstraZeneca, AbbVie, Merck, and Pfizer. D. Rasco is a consultant/advisory board member for TaiRm. R. Beckmann has ownership interest (including patents) in Eli Lilly and Company. T.S. Nguyen has ownership interest (including patents) in Eli Lilly and Company. M. Frenzel has ownership interest (including patents) in Eli Lilly and Company. D.M. Cronier has ownership interest (including patents) in Eli Lilly and Company. E.M. Chan has ownership interest (including patents) in Eli Lilly and Company. G.I. Shapiro reports receiving a commercial research grant from Eli Lilly and Company and other commercial research support from Pfizer, and is a consultant/advisory board member for Eli Lilly and Company, G1 Therapeutics, Vertex Pharmaceuticals, and Syros Pharmaceuticals. No potential conflicts of interest were disclosed by the other authors.

Authors' Contributions

Conception and design: A. Patnaik, L.S. Rosen, A.W. Tolcher, A. Nasir, R.P. Beckmann, A.D. Fulford, P. Kulanthaivel, L.Q. Li, D.M. Cronier, E.M. Chan, K.T. Flaherty, P.Y. Wen, G.I. Shapiro

Development of methodology: A. Patnaik, L.S. Rosen, A.W. Tolcher, J.W. Goldman, L. Gandhi, A. Nasir, A.D. Fulford, P. Kulanthaivel, L.Q. Li, E.M. Chan, G.I. Shapiro

Acquisition of data (provided animals, acquired and managed patients, provided facilities, etc.): A. Patnaik, L.S. Rosen, S.M. Tolaney, A.W. Tolcher, J.W. Goldman, L. Gandhi, K.P. Papadopoulos, D.W. Rasco, J.F. Hilton, A. Nasir, R.P. Beckmann, A.E. Schade, R. Martinez, E.M. Chan, K.T. Flaherty, P.Y. Wen, G.I. Shapiro

Analysis and interpretation of data (e.g., statistical analysis, biostatistics, computational analysis): A. Patnaik, L.S. Rosen, J.W. Goldman, L. Gandhi, M. Beeram, J.F. Hilton, A. Nasir, R.P. Beckmann, A.E. Schade, T.S. Nguyen, R. Martinez, P. Kulanthaivel, L.Q. Li, M. Frenzel, D.M. Cronier, E.M. Chan, K.T. Flaherty, P.Y. Wen, G.I. Shapiro

Writing, review, and/or revision of the manuscript: A. Patnaik, L.S. Rosen, S.M. Tolaney, A.W. Tolcher, J.W. Goldman, L. Gandhi, K.P. Papadopoulos, J.F. Hilton, A. Nasir, R.P. Beckmann, A.E. Schade, A.D. Fulford, T.S. Nguyen, R. Martinez, P. Kulanthaivel, L.Q. Li, M. Frenzel, D.M. Cronier, E.M. Chan, K.T. Flaherty, P.Y. Wen, G.I. Shapiro

Administrative, technical, or material support (i.e., reporting or organizing data, constructing databases): A. Patnaik, A.W. Tolcher, L. Gandhi, A. Nasir, A.D. Fulford, L.Q. Li, M. Frenzel, D.M. Cronier, E.M. Chan, P.Y. Wen, G.I. Shapiro

Study supervision: A. Patnaik, L.S. Rosen, S.M. Tolaney, M. Beeram, L.Q. Li, E.M. Chan, G.I. Shapiro

Other (design of biomarker assay, training/supervision of CRO staff in analytical validation of the assays to evaluate modulation of PD biomarkers): A.D. Fulford

Acknowledgments

The authors thank the patients and families who participated in this study and the staff who cared for these patients at the investigative sites. Eli Lilly and Company funded the medical writing support provided by Stephanie Brillhart, who is an employee of inVentiv Health Clinical.

Grant Support

All funding was provided by Eli Lilly and Company.

Received January 20, 2016; revised April 22, 2016; accepted April 26, 2016; published OnlineFirst May 23, 2016.

REFERENCES

1. Weinberg RA. The retinoblastoma protein and cell cycle control. Cell 1995;81:323–30.
2. Morgan DO. Principles of CDK regulation. Nature 1995;374:131–4.
3. Carnero A, Hannon GJ. The INK4 family of CDK inhibitors. Curr Top Microbiol Immunol 1998;227:43–55.
4. Sherr CJ, Roberts JM. CDK inhibitors: positive and negative regulators of G1-phase progression. Genes Dev 1999;13:1501–12.
5. Sherr CJ, Beach D, Shapiro GI. Targeting CDK4 and CDK6: from discovery to therapy. Cancer Discov 2016;6:1–15.
6. Hall M, Peters G. Genetic alterations of cyclins, cyclin-dependent kinases, and CDK inhibitors in human cancer. Adv Cancer Res 1996;68:67–108.
7. Sherr CJ. Cancer cell cycles. Science 1996;274:1672–7.
8. Shapiro GI. Cyclin-dependent kinase pathways as targets for cancer treatment. J Clin Oncol 2006;24:1770–83.
9. Anders L, Ke N, Hydbring P, Choi YJ, Widlund HR, Chick JM, et al. A systematic screen for CDK4/6 substrates links FOXM1 phosphorylation to senescence suppression in cancer cells. Cancer Cell 2011;20:620–34.
10. Zou X, Ray D, Aziyu A, Christov K, Boiko AD, Gudkov AV, et al. CDK4 disruption renders primary mouse cells resistant to oncogenic transformation, leading to Arf/p53-independent senescence. Genes Dev 2002;16:2923–34.
11. Yu Q, Geng Y, Sicinski P. Specific protection against breast cancers by cyclin D1 ablation. Nature 2001;411:1017–21.
12. Reddy HK, Mettus RV, Rane SG, Grana X, Litvin J, Reddy EP. Cyclin-dependent kinase 4 expression is essential for neu-induced breast tumorigenesis. Cancer Res 2005;65:10174–8.
13. Yu Q, Sicinska E, Geng Y, Ahnstrom M, Zagozdzon A, Kong Y, et al. Requirement for CDK4 kinase function in breast cancer. Cancer Cell 2006;9:23–32.
14. Puyol M, Martin A, Dubus P, Mulero F, Pizcueta P, Khan G, et al. A synthetic lethal interaction between K-Ras oncogenes and Cdk4 unveils a therapeutic strategy for non-small cell lung carcinoma. Cancer Cell 2010;18:63–73.
15. Choi YJ, Li X, Hydbring P, Sanda T, Stefano J, Christie AL, et al. The requirement for cyclin D function in tumor maintenance. Cancer Cell 2012;22:438–51.
16. Serrano M, Gomez-Lahoz E, DePinho RA, Beach D, Bar-Sagi D. Inhibition of ras-induced proliferation and cellular transformation by p16INK4. Science 1995;267:249–52.
17. Malumbres M, Sotillo R, Santamaria D, Galan J, Cerezo A, Ortega S, et al. Mammalian cells cycle without the D-type cyclin-dependent kinases Cdk4 and Cdk6. Cell 2004;118:493–504.
18. Kozar K, Ciemerych MA, Rebel VI, Shigematsu H, Zagozdzon A, Sicinska E, et al. Mouse development and cell proliferation in the absence of D-cyclins. Cell 2004;118:477–91.
19. Sherr CJ, Roberts JM. Living with or without cyclins and cyclin-dependent kinases. Genes Dev 2004;18:2699–711.
20. Malumbres M, Barbacid M. Cell cycle, CDKs and cancer: a changing paradigm. Nat Rev Cancer 2009;9:153–66.
21. Gelbert LM, Cai S, Lin X, Sanchez-Martinez C, Del PM, Lallena MJ, et al. Preclinical characterization of the CDK4/6 inhibitor LY2835219: in-vivo cell cycle-dependent/independent anti-tumor activities alone/in combination with gemcitabine. Invest New Drugs 2014;32:825–37.
22. Tate SC, Cai S, Ajamie RT, Burke T, Beckmann RP, Chan EM, et al. Semi-mechanistic pharmacokinetic/pharmacodynamic modeling of the antitumor activity of LY2835219, a new cyclin-dependent kinase 4/6 inhibitor, in mice bearing human tumor xenografts. Clin Cancer Res 2014;20:3763–74.
23. Yadav V, Burke TF, Huber L, Van Horn RD, Zhang Y, Buchanan SG, et al. The CDK4/6 inhibitor LY2835219 overcomes vemurafenib resistance resulting from MAPK reactivation and cyclin D1 upregulation. Mol Cancer Ther 2014;13:2253–63.
24. Raub TJ, Wishart GN, Kulanthaivel P, Staton BA, Ajamie RT, Sawada GA, et al. Brain exposure of two selective dual CDK4 and CDK6 inhibitors and the antitumor activity of CDK4 and CDK6 inhibition in combination with temozolomide in an intracranial glioblastoma xenograft. Drug Metab Dispos 2015;43:1360–71.
25. Caldon CE, Daly RJ, Sutherland RL, Musgrove EA. Cell cycle control in breast cancer cells. J Cell Biochem 2006;97:261–74.
26. Finn RS, Dering J, Conklin D, Kalous O, Cohen DJ, Desai AJ, et al. PD 0332991, a selective cyclin D kinase 4/6 inhibitor, preferentially

inhibits proliferation of luminal estrogen receptor-positive human breast cancer cell lines in vitro. Breast Cancer Res 2009;11:R77.
27. Van Allen EM, Wagle N, Stojanov P, Perrin DL, Cibulskis K, Marlow S, et al. Whole-exome sequencing and clinical interpretation of formalin-fixed, paraffin-embedded tumor samples to guide precision cancer medicine. Nat Med 2014;20:682–8.
28. Skoulidis F, Byers LA, Diao L, Papadimitrakopoulou VA, Tong P, Izzo J, et al. Co-occurring genomic alterations define major subsets of KRAS-mutant lung adenocarcinoma with distinct biology, immune profiles, and therapeutic vulnerabilities. Cancer Discov 2015;5:860–77.
29. Nam EJ, Kim YT. Alteration of cell-cycle regulation in epithelial ovarian cancer. Int J Gynecol Cancer 2008;18:1169–82.
30. Rustin GJ, Vergote I, Eisenhauer E, Pujade-Lauraine E, Quinn M, Thigpen T, et al. Definitions for response and progression in ovarian cancer clinical trials incorporating RECIST 1.1 and CA 125 agreed by the Gynecological Cancer Intergroup (GCIG). Int J Gynecol Cancer 2011;21:419–23.
31. Cancer Genome Atlas Research Network. Comprehensive genomic characterization defines human glioblastoma genes and core pathways. Nature 2008;455:1061–8.
32. Dai CY, Furth EE, Mick R, Koh J, Takayama T, Niitsu Y, et al. p16(INK4a) expression begins early in human colon neoplasia and correlates inversely with markers of cell proliferation. Gastroenterology 2000;119:929–42.
33. Sheppard KE, McArthur GA. The cell-cycle regulator CDK4: an emerging therapeutic target in melanoma. Clin Cancer Res 2013;19:5320–8.
34. Schwartz GK, LoRusso PM, Dickson MA, Randolph SS, Shaik MN, Wilner KD, et al. Phase I study of PD 0332991, a cyclin-dependent kinase inhibitor, administered in 3-week cycles (Schedule 2/1). Br J Cancer 2011;104:1862–8.
35. Flaherty KT, LoRusso PM, Demichele A, Abramson VG, Courtney R, Randolph SS, et al. Phase I, dose-escalation trial of the oral cyclin-dependent kinase 4/6 inhibitor PD 0332991, administered using a 21-day schedule in patients with advanced cancer. Clin Cancer Res 2012;18:568–76.
36. Finn RS, Crown JP, Lang I, Boer K, Bondarenko IM, Kulyk SO, et al. The cyclin-dependent kinase 4/6 inhibitor palbociclib in combination with letrozole versus letrozole alone as first-line treatment of oestrogen receptor-positive, HER2-negative, advanced breast cancer (PALOMA-1/TRIO-18): a randomised phase 2 study. Lancet Oncol 2015;16:25–35.
37. Turner NC, Ro J, Andre F, Loi S, Verma S, Iwata H, et al. Palbociclib in hormone-receptor-positive advanced breast cancer. N Engl J Med 2015;373:209–19.
38. Kim S, Loo A, Chopra R, Caponigro G, Huang A, Vora S, et al. LEE011: an orally bioavailable, selective small molecule inhibitor of CDK4/6 reactivating Rb in cancer. Mol Cancer Ther 12[11S:PRO2]. 2013.
39. Infante JR, Shapiro GI, Witteveen P, Gerecitano JF, Ribrag V, Chugh R. Phase 1 multicenter, open label, dose-escalation study of LEE011, an oral inhibitor of cyclin-dependent kinase 4/6, in patients with advanced solid tumors or lymphomas. Mol Cancer Ther 2013;12 (11 suppl; abstr A276).
40. Guan JL, Zhong WZ, An SJ, Yang JJ, Su J, Chen ZH, et al. KRAS mutation in patients with lung cancer: a predictor for poor prognosis but not for EGFR-TKIs or chemotherapy. Ann Surg Oncol 2013;20:1381–8.
41. Calles A, Sholl LM, Rodig SJ, Pelton AK, Hornick JL, Butaney M, et al. Immunohistochemical loss of LKB1 is a biomarker for more aggressive biology in KRAS-mutant lung adenocarcinoma. Clin Cancer Res 2015;21:2851–60.
42. Chen Z, Cheng K, Walton Z, Wang Y, Ebi H, Shimamura T, et al. A murine lung cancer co-clinical trial identifies genetic modifiers of therapeutic response. Nature 2012;483:613–7.
43. DeMichele A, Clark AS, Tan KS, Heitjan DF, Gramlich K, Gallagher M, et al. CDK 4/6 inhibitor palbociclib (PD0332991) in Rb+ advanced breast cancer: phase II activity, safety, and predictive biomarker assessment. Clin Cancer Res 2015;21:995–1001.
44. Sharpless NE, Sherr CJ. Forging a signature of in vivo senescence. Nat Rev Cancer 2015;15:397–408.
45. Eisenhauer EA, Therasse P, Bogaerts J, Schwartz LH, Sargent D, Ford R, et al. New response evaluation criteria in solid tumours: revised RECIST guideline (version 1.1). Eur J Cancer 2009;45:228–47.
46. Kaplan EL, Meier P. Nonparametric estimation from incomplete observations. J Am Stat Assoc 1958;53:457–81.
47. Brosh R, Rotter V. When mutants gain new powers: news from the mutant p53 field. Nat Rev Cancer 2009;9:701–13.